1   **Field sampling of soil pore water to evaluate the mobile fraction of trace elements in the**

2   **Iglesiente area (SW Sardinia, Italy)**

3

4   *Sara Concas[1], Carla Ardau[1]*, Marcello Di Bonito[2], Pierfranco Lattanzi[1], Andrea Vacca[1]*

5   *1.   Dipartimento di Scienze chimiche e geologiche, Università di Cagliari, Italy*

6   *2.   School of Animal, Rural, and Environmental sciences, Nottingham Trent University, UK*

7   **corresponding author: carla.ardau@tiscali.it*

8

9   **Abstract**

10 Field soil pore water monitoring was applied in a highly heavy-metal contaminated area in SW

11 Sardinia, Italy, as a direct, realistic measure of heavy metal mobility. The main chemistry of pore

12 waters well reflects the local characteristics of soils, ranging from $Ca-SO_4$ to $(Ca)Mg-HCO_3$ to

13 $Ca(Na)-SO_4(Cl)$, with a wide range of conductivity. The mobility of Zn and Pb is apparently

14 controlled by equilibrium with minerals such as hydrozincite or smithsonite, and cerussite,

15 respectively. These results allow a correct estimate of the actual environmental risk associated with

16 the presence of heavy metals in soils, and may serve as a supporting tool for phytoremediation

17 planning.

18

19 **Key words**: soil pore water; heavy metal mobility; Iglesiente (Sardinia)

20

21 **1. Introduction**

22 The presence of potentially toxic chemical elements (PTEs) in soils, either naturally occurring or

23 from anthropogenic activities (such as, amongst others, mining activity), represents a serious

24 environmental threat, involving the entire system of relationships between hydrosphere, geosphere

25 and biosphere (Nkongolo et al., 2013; Li et al., 2014). In the past century, mining was the driving

26 sector of the economy in south-western Sardinia (Italy). Mining industry began to decline around

27 the end of the century, leading to the closure of most mines over the 1970–1990 period. There are

28 now in the region about 170 abandoned mines, and 200 million tons of mining-related wastes,

29   covering a surface of 19 km^2 (RAS, 2003; Ardau et al., 2013). Due to the ineffective or totally

30   absent management of mining-related wastes in the last decades, in several Sardinian areas the PTE

31   contamination extended to the surrounding environment, affecting air, water and soils (e.g. Aru et

32   al., 1995; Vacca & Vacca, 2001; Cidu et al., 2001; Concas et al., 2006; Cidu et al., 2011; Fanfani &

33   Ardau, 2011; Vacca et al., 2012; Cidu et al., 2012; Ardau et al., 2013).

34   In abandoned mining areas, removal, treatment or confinement of mining-related wastes may

35   be not viable for several practical reasons, including the extremely high costs (Lomelin, 2002;

36   González et al., 2006; Ardau et al., 2013). A 'soft' alternative is represented by phytoremediation

37   (Barbafieri et al., 2011), that includes two different options: phytostabilization and phytoextraction

38   (Chaney et al., 1997). Phytoextraction may represent a valuable, cost-effective alternative to

39   traditional disruptive technologies (Cao et al., 2007), but it is often of limited application. A more

40   widely applicable technique is phytostabilization, because the quick establishment of a dense

41   vegetation cover is crucial to limit wind and water erosion. Moreover, plant roots may immobilize

42   metals by adsorption or accumulation, and provide a rhizosphere wherein metals precipitate and

43   stabilize (Mendez & Maier 2008; Cao et al., 2009; Nicoară et al., 2014).

44   One of the prerequisites for phytoremediation planning and management is to identify mobility and

45   phytoavailable fraction of (toxic) chemical components in soil/wastes. From many studies

46   (Impelliteri et al., 2003; Tye et al., 2003; Cui et al., 2014), it is well established that total soil/waste

47   metal content alone is not an adequate measure of the potential mobility of a (toxic) element and,

48   consequently, of its possible uptake by plants (Vig et al., 2003; Di Bonito et al., 2008; Barbafieri et

49   al, 2011). Therefore, chemical methods to determine trace metal phytoavailability in soils are

50   usually based on the measurement of the extractable or labile fractions of those elements (De Siervi

51   et al., 2004). However, there is no agreement on how to evaluate at best the risk arising from the

52   fraction of pollutants that are most mobile in soils (Sneddon et al., 2006; Vázquez et al., 2008;

53   Moreno-Jiménez et al., 2011). Among the possible methods of identification, the direct

54   measurement of the composition of soil pore waters is being increasingly applied, due to many

55   advantages in term of simplicity and costs (Meers et al., 2007; Di Bonito et al., 2008; Beesley et al.,

56   2010; Moreno-Jiménez et al., 2011; Shaheen et al., 2014).

57   In the present study, the composition (major element chemistry and selected heavy metal

58   contents) of soil pore water was determined in a highly heavy-metal contaminated area included in

59   the Iglesiente mining district (south-western Sardinia, Italy), one of the largest of the island, and of

60   importance at the European scale. To the best of authors' knowledge, this is the first time that this

61   technique is applied in the district. The study area is located in a geographic region with a typically

62   Mediterranean climate, with very dry summers, and is characterized by natural geochemical

63   anomalies (particularly Pb, Zn, Ba), enhanced by centuries of mining activity (Bechstädt et al.,

64   1994; Boni et al., 1999). The monitoring of temporal, local and spatial variations in pore water

65   quantity and quality was carried on from a series of undisturbed soil/mine waste profiles. The study

66   is a significant part of a more extended project (Concas, 2014). In a companion paper (Concas et al.,

67   submitted), the metal uptake by an endemic Mediterranean species (*Pistacia lentiscus* L.) was

68   assessed. Although not part of this specific paper, some recall to that supplementary information

69   will be made for a more robust data discussion.

70

71   **2. Materials and methods**

72   *2.1 Study site*

73   The Iglesiente mining district (Sardinia, Italy) was for centuries up to the 1990s the seat of intense

74   mining activity. The ore bodies are hosted in Cambrian dolomites and limestones, and produced

75   some hundred million tons of Zn–Pb–Ag and Ba ores (Boni et al., 1999, and references therein).

76   The cessation of mining activity left large quantities of mine wastes in dumps and flotation tailings

77   basins, estimated at about 45 million m^3 for the whole area (Cao et al., 2009).

78   Concas (2014) describes a total of 9 soil profiles in 5 sites in the basin of the San Giorgio river,

79   having an extension of about 2,563 ha (Fig.1). Four main representative sites were selected for this

80   study. The first site *(Campo Pisano)* is located near the town of Iglesias, the main urban centre of

the area. Campo Pisano is one of the hazard centres of the district because of the presence of waste impoundments where, during mining activity in the 1900s, flotation wastes from several mines of the district were collected, in particular from Monteponi mine (Cidu et al., 2001, RAS, 2003). The flotation wastes (about 8 million m^3) contain Pb and Zn as the most abundant heavy metals. Due to the high heavy metal concentrations, low organic carbon, and low cation exchange capacity, the flotation wastes area appears bare and unvegetated (Cao et al., 2009). Specifically, samples for this study (sampling points P1 and P3 in Fig. 1) were collected from two different experimental plots used for a previous revegetation test with endemic species (*Pistacia lentiscus* L.; Bacchetta et al., 2012). P1 samples are from a plot representing the untreated waste material, while P3 samples are from a plot where some compost was added. Since planting in 2008, *P. lentiscus* survived only in the P3 plot (Fig. 2).

The second and third sampling areas are two natural sites, not visibly affected by morphological alterations due to mineral extraction, located in the natural substrate of Cambrian limestones and dolostones, that host the metalliferous bodies (sampling points P5 - *Serra Merareddu,* and P6 - *Pozzo Santa Barbara* - Fig. 1). These sites, characterised by natural geochemical anomalies (particularly in Zn and Pb), though not intended to statistically represent the whole district, can give an idea of pre-mining conditions. In both sites *P. lentiscus* grows spontaneously. The fourth site is a lagoon deposit at *Sa Masa*, near the Funtanamare beach (sampling point P9 in Fig.1), final collector of waters and pollutants from the entire watershed of the San Giorgio river (including mining seepages, and sewage waters from the Iglesias town). Therefore, the high contamination at Sa Masa (see below) is not just site specific, but induced by transportation of solid and liquid matrixes from other localities within the San Giorgio basin. Even at Sa Masa, *P. lentiscus* grows spontaneously.

As previously noted, the climate of the area is typically Mediterranean, characterised by very dry summers. The maximum annual average temperature is 25°C, and the minimum 5°C. Average annual precipitation is ca. 800 mm (http://my.meteonetwork.it/station/srd025/statistiche).

107   *2.2 Soil characterization*

108   At each study site, a soil profile was opened and described, making a distinction in pedogenetic

109   horizons according to standard procedures of soil description (Schoeneberger et al., 2002); samples

110   of each horizon were collected for subsequent laboratory analyses. Even though Campo Pisano is

111   not classifiable as natural soil, for descriptive purposes the terms 'soil' and 'soil horizon' are also

112   used for that site, where the substrate is in fact mainly composed of mine tailings. This study

113   considers data from shallow, unsaturated horizons, according to the lysimeter or rhizometer depths

114   used for field soil pore-water extraction (see below). The complete set of soil data is available in

115   Concas (2014).

116   Bulk soil samples were air-dried and sieved (<2 mm, fine earth). Routine physical and chemical

117   analyses were carried out according to the procedures published by the Italian Ministry of

118   Agriculture (MiPAF, 1998, 2000). Sand (2.00–0.05 mm), silt (0.050–0.002 mm) and clay (<0.002

119   mm) fractions were separated after the removal of organic matter by H_2O_2 treatment and dispersion

120   aided by Na-hexametaphosphate by the sieve and pipette methods. The soil pH was measured in a

121   1:2.5 soil/water suspension. The organic carbon (OC) was estimated by wet digestion with a

122   modified Walkley–Black procedure. Soils were classified according to IUSS Working Group WRB

123   (2014). Mineralogical analyses were performed on the <2 mm fraction by powder X-ray diffraction

124   (PXRD), on an automated Panalytical X'pert Pro diffractometer with Ni-filter Cu-$K_{\alpha 1}$ radiation (λ =

125   1.54060 Å), operating at 40 kV and 40 mA, using the X'Celerator detector (see 4.1 paragraph). The

126   main soil chemical components (major element oxides for ordinary rocks) were also determined on

127   the <2 mm fraction by a Philips PW1480 wavelength-dispersive X-ray fluorescence (WDXRF). For

128   the A horizon at the P9 location, it was not possible to obtain a suitable pellet for XRF analysis,

129   because of its loose incoherent texture. Information on its 'major oxide' content is not critical for

130   the purposes of this paper, and we made no further efforts to obtain these data. Raw intensities were

131   corrected for matrix effects by the method of Franzini & Leoni (1972), making reference to

132   certified rock standards. The method is calibrated for ordinary rocks, with comparatively low heavy

metal contents. The correction routine does not adequately account for the unusually high contents of Pb and Zn typical of most of our samples. Therefore, XRF data should be taken as semi-quantitative. Loss of ignition (LOI) was determined by leaving an aliquot of the sample at 900°C for 8 hrs, and expressed as percent weight difference before and after the treatment. Contributions to LOI include carbonate decomposition, dehydration of clay minerals and/or Fe-Al oxyhydroxides, and burning of organic matter. The total heavy metal contents of soil samples were determined on the <2 mm fraction after digestion in microwave system (Milestone Ethos 1 oven) with a $HNO_3/HF/HClO_4$ (5:2:1 v/v) mixture, as proposed by Brunori et al. (2005), analysing the obtained solutions by an inductively coupled plasma optical emission spectrometer (ICP-OES Analyzer, ARL Fisons 3520B). Soil samples were randomly digested and analysed in replicate to test the precision of the method. In this case the average datum of the two aliquots was considered. The accuracy was tested against the certified standard NIST 2710. Overall, heavy metal analyses in soils are within $\pm$10% for both accuracy and precision.

2.3 Soil pore water sampling and analyses

At each study site soil pore water samples were collected from unsaturated profiles, in the rooting zone. In order to reduce as much as possible soil disturbance during sample collection SPS 200 soil water samplers (SDEC, France) were used (Lekakis et al., 2015). The samplers, namely 'vacuum lysimeters', are characterised by a porous ceramic cup glued on the bottom of an empty PVC tube (31 mm in diameter), and are designed to replicate the suction function of plant roots.

The samplers were placed in all sampling points at 10-15 cm depth into the upper soil horizon, and, when possible, at 30-40 cm depth into the underlying horizon. At P1 and P3, only short lysimeters were used, because of the shallow depth of soils. Before starting the sampling, the lysimeters were left for 1 month in the field to equilibrate. One day before sampling, a vacuum of -75 kPa was created inside the tube with a vacuum pump (SPS400, SDEC, France), through a connecting tube hosted in a pierced rubber bung, in order to draw the pore water from the soil to the porous ceramic

cup and into the tube. To sample the pore water, the vacuum pump was used to collect the soil solution contained in the tube, which was then poured into a sampling flask. Because of the climate of the area, with very dry summers, four surveys were carried out between the rainiest period, corresponding to the winter, and the starting of the dry season (from December 2012 to April 2013). In fact, fall 2012 was unusually dry, and at the time of the first sampling (December 2012) it was possible to obtain enough liquid for analysis only at Campo Pisano and Sa Masa. In the following months (January − February 2013), there was enough rain infiltration to allow collection of sufficient pore water from most lysimeters. In April 2013, with the beginning of the dry season, only at Sa Masa, where the water table was always shallow, it was possible to collect soil pore water. At this site in April 2013 three additional samples were collected using another type of tension sampler, namely the 'rhizon sampler' or 'rhizometer' (Eijkelkamp Agrisearch Equipment, The Netherlands) (Tye et al., 2003; Di Bonito et al., 2008). Using this device, pore water solution is extracted by inserting it into the soil, and connecting a syringe for applying the vacuum and then a suction. Sampling points were two at Campo Pisano (sampling points 1 and 2, respectively at P1 and P3), three at the Serra Merareddu (P5) site (sampling points 6a, 6b and 6c), where letters a, b …indicate that lysimeters were positioned all around the same *P. lentiscus* individual*;* three at the Pozzo Santa Barbara (P6) site (sampling points 7a, 7b and 7c), and eight at the Sa Masa (P9) site, respectively five sampled by lysimeters (sampling points 4a, 4b, 4c and 5a, 5b), two by rhizometer (sampling points 19 and 22), and one sampled by both (sampling point 25).

Pore waters collected with lysimeters were filtered to 0.45 μm; for solutions extracted by rhizon samplers this filtering is not necessary, because their porosity is less than 0.45 μm. Labile parameters (temperature, pH, conductivity) were measured in the field. Because of the scarcity of collected liquid, Eh was not routinely determined; in the few samples where it was measured, the values indicate oxidising conditions (equilibrium with the atmosphere), as expected for unsaturated horizons. The solutions were stabilised to 1% v/v with HNO_3 for the subsequent analyses of major and trace elements, including heavy metals. Whenever enough solution was available, total

185   alkalinity was determined independently by HCl titration on another aliquot. The major elements

186   were measured by Ion Chromatography, and the trace elements (Zn, Pb, Cd, Mn, Fe, Cu) by ICP-

187   OES (Perkin Elmer Optima 2100 DV). Because of solution scarcity, anions were determined on the

188   same acidified aliquot used for cations; obviously, this made impossible the measure of nitrate in

189   solution. In Sardinia, high (>50 mg/L) nitrate content in groundwaters is mostly linked to

190   agriculture (RAS, 2010), which is not the land use of any of the studied sites. Moreover, ionic

191   charge balances (see below) do not suggest anion deficit in any of the analyzed pore waters. In

192   some cases (data marked with * in Tables 3a and 3b), when the solution from a single sampling was

193   not sufficient for the analyses, pore waters from two close sampling points were combined.

194   The dissolved organic carbon (DOC) was determined by TOC/TN analyser (Analytical Sciences

195   Thermalox program), a specific instrument for total organic carbon and nitrogen contents in water

196   solutions. The instrument actually determines the total carbon (TC); whereas the dissolved

197   inorganic (carbonate) carbon (DIC) is removed by acid addition, and the remaining DOC is

198   measured by a second pass in the TOC analyser. The inorganic carbon is calculated as the

199   difference between TOC and DOC. When it was not possible to collect enough pore water for an

200   independent determination of alkalinity, the value of DIC was used to calculate alkalinity as HCO_3^-.

201   Quality control of pore water chemical analyses is intrinsically difficult. To the best of authors'

202   knowledge, there are no specific certified international standards, and replicate analyses were

203   seldom possible. Preliminary release tests with deionised water on new lysimeters and rhizometers

204   indicated negligible (below detection limits for ICP-OES) amounts of released elements, except for

205   Ba. For this element, high values were recorded in lysimeter blanks, therefore data for Ba were not

206   included in this study. Field blanks were obtained by introducing deionised water in the same

207   devices used for pore water samples, and treating the collected volumes as independent samples.

208   The accuracy of ICP-OES analyses was checked with calibration standard solutions. A further

209   check of quality of analysis for major elements are ionic balances. From data in Table 3b, it is

210 possible to calculate ionic balances: most are within $\pm10\%$, and only two are within $\pm15\%$. Overall,

211 it is estimated that most of analyses are within $\pm20\%$ error for both accuracy and precision.

212 The collected data were elaborated with two different speciation programs, PHREEQC 3.0.2

213 (Parkhurst et al., 1980; Parkhurst, 1995) and WHAM 7.0.2 (Tipping, 1994); specifically, the second

214 accounts for complexation of metals by organic matter.

215

216 **3. Results**

217

218 *3.1 Soil characterization*

219 Field observations, summarized in Table 1, showed that (i) the soil derived from untreated waste

220 material (P1) is shallow, and characterized by a very thin cemented and hardened surface horizon

221 overlying two mineral horizons slightly enriched in organic carbon (OC); (ii) the soil derived from

222 the waste material treated with compost (P3) is shallow, and characterized by a ploughed epipedon

223 enriched in OC; (iii) soils derived from dolomitic limestones (P5 and P6) are shallow or moderately

224 deep, with A horizon at surface and a well expressed Bw horizon, and lithic contact toward the

225 underlying bedrock; (iv) the soil derived from Holocene lagoon deposits at Sa Masa (P9) is deep,

226 and characterized by a sequence of different sedimentary cycles (marked by differences in texture).

227 The differences in texture among the soils (Table 1) reflect their origin from different parent

228 materials, and confirm the field assessment. Reaction is generally neutral to slightly alkaline, with

229 the exception of the strongly acid 2^C horizon of P1 and P3, and the moderately alkaline 5C4 and

230 6C5 horizons of P9. OC contents are highest in the surface horizons and decrease regularly with

231 depth.

232 In the World Reference Base (WRB), the studied soils classify as follows: Spolic Technosol (P1

233 and P3), Endoleptic Luvisol (Abruptic, Humic, Clayic, Rhodic) (P5), Epileptic Luvisol (Abruptic,

234 Humic, Chromic) (P6), and Haplic Fluvisol (Calcaric, Ruptic) (P9).

235   The main physicochemical characteristics of the studied soils are reported in Table 1, while

236   mineralogical composition is described hereafter. At Campo Pisano (P1 and P3), tailings

237   mineralogy is dominated by the presence of quartz, gypsum and carbonates (mainly dolomite,

238   secondarily calcite and traces of ankerite), with minor muscovite and microcline, and residual

239   pyrite. Hydrozincite, cerussite, as well as traces of sphalerite and galena, were also detected in some

240   horizons.

241   Samples from Serra Merareddu (P5) and Pozzo Santa Barbara (P6) contain a clay component

242   (kaolinite and montmorillonite), as expected in *sensu stricto* soils. The main mineral at both sites is

243   however quartz (possibly of aeolic deposition: Concas, 2014). Dolomite is the predominant

244   carbonate; barite occurs in all profiles. At Sa Masa (P9), carbonates (calcite, dolomite, and

245   subordinate ankerite) and quartz represent the main minerals. Minor minerals include

246   hemimorphite, barite, and cerussite. As observed above, at Sa Masa some mineral component could

247   result from transport from other localities.

248   The main chemical composition (Table 2a) is substantially in agreement with the mineralogy of

249   soils. High LOI and CaO values in samples from Campo Pisano and Sa Masa are indicative of the

250   presence of a major carbonatic fraction, while in P5 and P6 profiles the prevalence of the quartz and

251   phyllosilicate fraction is well pinpointed by high values of SiO_2 and Al_2O_3. Iron (as Fe_2O_3) is

252   significant, as expected, in the tailing samples from Campo Pisano (P1 and P3), where, other than in

253   residual pyrite or ankerite, it could be also present as poorly crystalline Fe-oxide-hydroxides from

254   sulphides oxidation, such as ferrihydrite (Blowes et al., 2003; Marescotti et al., 2012; Ardau et al.,

255   2014), not easily identifiable by PXRD analyses in complex matrixes; the site with the lowest Fe is

256   Sa Masa.

257   Among heavy metals (Table 2b), Zn concentration is around thousand mg kg^{-1} at Pozzo S. Barbara

258   (P6), from thousand to ten thousand mg kg^{-1} at Campo Pisano (P1 and P3) and Serra Merareddu

259   (P5), from thousand to hundred thousand mg kg^{-1} at Sa Masa (P9). Lead concentrations vary from

260   thousand mg kg^{-1} at Campo Pisano and Pozzo S. Barbara, and from thousand to ten thousand at

261 Serra Merareddu and Sa Masa. Cadmium and Cu are present in amounts around tens mg kg^{-1} in all

262 sites, except at Sa Masa where concentrations can reach hundreds mg kg^{-1}.

263 As it can be observed from chemical results, the natural soils at P5 and P6 sites show heavy metal

264 contents of the same order of magnitude as the mining flotation waste at Campo Pisano. Some

265 values are in fact higher than median values of stream sediments in the district (Boni et al., 1999),

266 which can be taken as an indication of the local post-mining geochemical baseline. Concas (2014)

267 reports that at these sites the rock substrates (R layer) show appreciably lower metal contents,

268 suggesting that either the sites are in some way contaminated by anthropic activities (e.g., by wind

269 transport from nearby mine sites), and/or pedogenetic processes led to a (passive) enrichment in

270 some heavy metals. This issue is beyond the purpose of this paper, and it will not be further

271 discussed.

272

273 *3.2 Pore water chemistry*

274 The overall major element chemistry of pore water samples, distinguished for location, is depicted

275 in the Piper diagram of Fig. 3. Tables 3a and 3b and 4a and 4b report the main physical and

276 chemical parameters (including major and selected trace components) of the studied pore waters,

277 divided for location and sampling periods.

278 Fig. 3 points out a clear difference among pore water major chemistry of Campo Pisano samples

279 (P1 and P3) from the natural substrate of Cambrian limestones and dolostones (P5 and P6), and

280 from Sa Masa (P9). In terms of descriptive hydrochemical facies (e.g., Back, 1966), the Campo

281 Pisano waters belong to a Ca-SO$_4$ type, those of P5 and P6 to a Mg-HCO$_3$ type (with a subordinate

282 Cl component for some samples), and those at Sa Masa again to a Ca-SO$_4$ type, but with a

283 significant Na-Cl component, presumably reflecting a marine input, either from seawater ingression

284 or from sea spray deposition (see further discussion).

285 Conductivity of pore waters is highly variable, ranging from ~570-900 μS cm^{-1} in samples from the

286 natural substrate, ~1200-2000 μS cm^{-1} at Campo Pisano, up to ~2400-3700 μS cm^{-1} at Sa Masa,

287 indicating that the overall amount of soluble minerals, influencing pore water components, is rather

288 different in the three sites. Moreover, at Sa Masa a direct influence of the sea water component (see

289 below) in the high conductivity is likely. The pH of pore waters shows a moderate range of

290 variation (from circumneutral to alkaline) for different sites and/or different sampling times.

291 With respect to trace elements, zinc presents the highest concentration at Sa Masa, in the order of

292 thousand $\mu g\ L^{-1}$, in particular at the deepest levels (up to 5700 $\mu g\ L^{-1}$, with the only exception of the

293 December 2012 sampling, when Zn does not exceed hundreds $\mu g\ L^{-1}$). At Campo Pisano, Zn

294 concentrations are around hundreds $\mu g\ L^{-1}$ (no substantial differences are observed between plots

295 P1 and P3). As observed at Sa Masa, concentrations are one order of magnitude lower during

296 December 2012 sampling. The lowest Zn concentration (averagely of tens $\mu g\ L^{-1}$) is recorded at P5

297 and P6, where December 2012 sampling was not possible for the absence of sufficient water (see §

298 2.3).

299 Lead concentrations are in the order of tens $\mu g\ L^{-1}$ in all sampling sites, in agreement with the

300 known low mobility of this metal at pH values >7. The highest concentrations are registered in

301 January 2013 at Serra Merareddu, which is also the site with the highest total Pb values in the soil.

302 Manganese concentrations may show a certain variability in samples of the same site (e.g. 4a, 4b,

303 4c); in general, this metal is more abundant at Sa Masa (up to hundreds $\mu g\ L^{-1}$). At Campo Pisano

304 Mn does not exceed tens of $\mu g\ L^{-1}$, while it is close or below the limit of detection in the natural

305 soils (P5 and P6).

306 Iron does not show high mobility, in spite, for example, of significant bulk soil concentrations at

307 Campo Pisano. In fact, as expected at pH values measured in the pore waters, Fe results strongly

308 bound to the solid fraction of the soil (e.g. Ardau et al., 2009), and therefore, often below the

309 detection limit in the pore water. When detectable, the saturation index ($SI^{[1]}$) modelling results (not

310 shown) indicate high oversaturation with respect to the most abundant Fe-oxide-hydroxide in

[1] Saturation index (SI) = log (IAP/K_{sp}), where IAP (ion activity product) is the product of the chemical activities of the dissolved ions of the mineral, and K_{sp} is the solubility product. SI shows whether a particular mineral is in equilibrium with solution (SI null), or will tend to dissolve (SI negative), or precipitate (SI positive)

mineralised areas, such as goethite or ferrihydrite. Iron is also the metal showing the highest local

variability as a function of sampling period (see for example P1), indicating a strict seasonality

relationship.

As expected from their comparatively low bulk soil concentrations, Cd and Cu are definitely

subordinate in pore waters of all sites.

The OC content varies from undetectable (<0.04 mg L^{-1}) up to 12.6 mg L^{-1} at Campo Pisano. OC

contents in pore waters are not clearly related to bulk OC in soils. Presumably, this finding reflects

different degrees of solubility of organic matter in the different sites.

Speciation equilibria, as calculated by PHREEQC and WHAM, are summarised in Table 5.

Calcium and Mg are mostly present as free ions (average 70-80% in all samples). In the natural

substrate (P5 and P6), Ca and Mg also show a subordinate association with carbonate species (CO_3

and HCO_3), while in sulphate-rich pore waters (Campo Pisano and Sa Masa) a subordinate

association with SO_4 is shown. As a general rule, all samples reach equilibrium or oversaturation

conditions with respect to calcite and dolomite (Fig 4a,b). Gypsum equilibrium is close to be

attained for samples from Sa Masa and Campo Pisano, while samples from natural substrate result

undersaturated with respect to it (Fig 4c).

Trace metals show a variety of species, the abundance of which is related either to the main water

composition, or to the specific behaviour of the element. $PbCO_3$, for example, is generally the most

abundant Pb species both in carbonate and in sulphate waters; a subordinate species for this metal is

$PbOH^+$. All samples are close or in equilibrium with cerussite (Fig. 4d), and undersaturated with

respect to anglesite (Fig. 4e).

Zinc mainly occurs as Zn^{2+} and subordinately as $ZnSO_4$. Several samples are close to equilibrium

with hydrozincite, but a few are strongly undersaturated (Fig. 4f). Hydrozincite was in fact

identified by PXRD in some samples. Smithsonite (Fig. 4g) is consistently undersaturated, but a

number of samples at Sa Masa are close to equilibrium with it. This mineral was never positively

recognized in the studied samples, but its widespread occurrence in the district is well documented.

Specifically, smithsonite has been recognized both in the 'red muds' tailings at Monteponi and at Campo Pisano, often in association with hydrozincite and hemimorphite (the so-called 'calamine' ores of the Iglesiente mining district were typically composed of Zn (hydroxy-) carbonates and silicates; Boni et al., 2003). Runoff from these wastes may well be transported to Sa Masa by the San Giorgio river.

Manganese occurs as free ion, or as ion pair with SO_4 and CO_3. Several pore waters are close to or above saturation with rhodocrosite (Fig. 4h). This phase was not recognized in the studied samples; alternatively, the phase(s) controlling Mn in pore waters could be solid solution(s) with calcite and/or dolomite.

Cadmium mainly occurs as $CdCl^+$ and Cd^{2+}, and copper as $CuCO_3$ and $CuOH^+$; moreover, this metal is the only one for which the fraction bound to colloidal fulvic acids (as calculated by the WHAM program) is important (up to 99%). It is difficult to identify the possible phases controlling the mobility of Cd and Cu, since these elements are presumably present as minor substituting ions both in primary and secondary phases, therefore they do not appear in mineral theoretical formulas as identified by the speciation program.

4. Discussion

This study supports field monitoring of soil pore water chemistry as a useful method to evaluate the environmental risk associated to the mobility of (toxic) elements. With respect to indirect methods (selective and/or sequential extractions), it is comparatively rapid, because it does not require the extraction step(s); moreover, it directly records field conditions, that may imply different metal mobilities in the same soil (as shown in this study by differences in sampling events at the same sites). An additional important aspect is that pore water chemistry well reflects the 'history' of the associated soil/waste, being not merely the expression of the local mineral and chemical composition of soil/waste, but also of its 'use', geographic and climatic context. In fact, from pore water data treatment emerged some distinctive marks to distinguish among the natural mineralised

363 soils, the mine waste 'soils', and the soil from a 'collecting' area, selected for this study. If

364 mineralogical composition is generally the main factor influencing pore water chemistry, an

365 interesting exception, linked to the geographic context, is represented by Sa Masa swamp soil. At

366 Sa Masa, the influence of the near sea in the main chemistry of pore water overlaps that of soil

367 mineralogy, while trace elements show the mark of the accumulated material from different mined

368 areas present in the S. Giorgio basin, in particular for the high presence of Zn, which turned out to

369 be the most mobile metal. Sa Masa site represents, therefore, a clear example on how the mere use

370 of the total metal content in order to evaluate potential environmental risk of a contaminated soil

371 may offer indication far from those obtained by the use of pore water.

372 At Campo Pisano (P1 and P3), we are not in presence of a *sensu stricto* soil, but the substrate is

373 composed of mining wastes. This nature of the 'soil' is well pointed out by a main chemistry

374 dominated by Ca-SO$_4$, reflecting the abundant presence of gypsum, secondary product of sulphide

375 oxidation (as a source of sulphate), and carbonates (as a source of calcium). The heavy metal

376 contents reflect their mobility at the pore water pH values (for example with a prevalence of Zn

377 with respect to Pb) and of their solid-speciation (see below).

378 In the natural substrate of Cambrian limestones and dolostones (P5 and P6), pore water chemistry

379 well marks the difference with respect to mined areas, mainly for a limited conductivity, indication

380 of a reduced reactivity of mineral phases. However, the field pore water is perfectly able to identify

381 the presence of a geochemically anomalous area. The main chemistry is dominated by the

382 carbonatic nature of the substrate, while sulphates, indicative of possible sulphide presence and of

383 their subsequent oxidation, are limited. The lower contents in Zn in pore waters from this site with

384 respect to Campo Pisano well reflect a limited reactivity of minerals in an undisturbed soil with

385 respect to a mining waste dump. Lead is an exception since, regardless of its total concentration in

386 soils, its pore water concentration is similar and comparatively low for all sites, probably because of

387 saturation with respect to cerussite.

388   In sites where lysimeters were positioned in more than one point (see paragraph 2.3), pore waters

389   variations in different sampling points are not significant, with the only exception of Mn. Variations

390   related to the sampling period were more significant. Salinity at Sa Masa was higher in December

391   2012, and lower in February and April 2013. As shown in Fig. 5, this trend of salinity variation is

392   matched by seasonal variations of both Na and Cl (and of SO_4 – not shown), suggesting that sea

393   water contributions prevail at this site. For lagoon deposits like Sa Masa, contributions of seawater

394   may be linked either to marine ingression, and/or to dissolution and infiltration of sea spray

395   deposited on the soil surface. Both phenomena are usually more pronounced during dry periods.

396   The input of sea salts from marine aerosol in groundwater (and surface water) close to the coast is a

397   well known phenomenon due to the dissolution by the rain of the particulate deposited on the

398   ground, and subsequent infiltration across the soil (e.g., Whipkey et al., 2000; Lorrai & Fanfani,

399   2007, and references therein). The current data may thus suggest that either marine ingression,

400   and/or sea spray infiltration increase the pore water marine component during drier seasons, whilst

401   pore water is subjected to a sort of 'dilution effect', affecting sea water components (and salinity)

402   during rainy periods, due to a washout of the first soil centimetres, and transportation of the soluble

403   sea component toward deeper horizons.

404   Compositional variations are also registered in the other sampling sites, as for example, Campo

405   Pisano. In this case the element variations are more linked to precipitation/dissolution of soluble

406   salts, effects of dilution, or possibly interaction time influence. In fact, under comparatively dry

407   conditions, circulation of soil fluids is not pervasive, and the system does not approach an

408   equilibrium state; another important aspect to be considered is that Zn, an essential micronutrient, is

409   constantly taken up by plants (including *P. lentiscus* – see below). Plant physiology is therefore at

410   the same time influencing and influenced by element concentration in soil pore water.

411   An added value of field pore water chemistry monitoring is also the possibility to perform element

412   speciation in solution, offering a further 'tile' for the understanding of interface processes between

413   hydrosphere and biosphere. In fact, as pinpointed by other authors (e.g. Moreno-Jiménez et al.,

414   2011 and references therein), the soluble fraction will interact differently with plant roots as a

415   function of element speciation; for instance Shahid et al. (2012, 2014) observed how organic

416   ligands are capable to modify Pb speciation by forming organo-metallic complexes of different

417   bioavailability. In this study we observe how the same concentration of some element in pore water

418   (e.g. Zn) could be characterised by differences in speciation at different sites/times. Though beyond

419   the purpose of this study, the understanding of how aqueous speciation may influence metal uptake

420   by *P. lentiscus* could be an interesting subject of further investigation. The associated use of

421   PHREEQC and WHAM programs also permitted to identify which heavy metals are preferentially

422   present as free ions or bound to colloidal fulvic acids, and possible speciation differences from site

423   to site.

424   In general, from equilibrium calculations, the soil/pore water contact time appears sufficient for

425   reaching equilibrium conditions with several mineral phases, mostly carbonates, present in the soil

426   (e.g. Ca-Mg carbonates, hydrozincite, cerussite, gypsum). This allows to evaluate which minerals

427   are mostly responsible for controlling element mobility. This control is not expected to vary in a

428   short time. However, if mineral abundance is expected to vary, e.g. because of alteration, it is

429   possible to hypothesise a change of pore water quality in medium/long-time term. This is

430   particularly true for 'soil' constituted by residual mining material as in Campo Pisano, more

431   subjected to rapid alteration.

432   A potential limitation of this field-based approach could be that, in Mediterranean climates, during

433   dry periods, pore water is not enough to be sampled, dictating and altering the sampling period

434   distribution depending on climatic conditions. However, information on variations due to seasonal,

435   climatic and morphological conditions is critical for the understanding of the physiological response

436   of plants in the geographic context in which they occur. Laboratory-based methods fail to supply

437   such information, and therefore long-term field studies, such as soil pore water monitoring, are

438   required.

439   In terms of environmental risk, the concentrations of metals in pore waters can be usefully

440   compared with limits established by Italian laws (D.lgs 152/2006) for subsurface waters (Tables 4a

441   and 4b). These limits are exceeded for Pb in most samples, and in many samples at P9 also for Zn,

442   Mn, and in three samples also for Cd; Mn limits are exceeded in some samples at Campo Pisano

443   (P1 and P3). Therefore, based on present data, there is a potential impact for heavy metals in the

444   area, especially at Sa Masa. It is interesting to notice that Campo Pisano, considered one of the

445   'hazard centres' of the district, does not show the highest levels of heavy metals neither in soils, nor

446   in pore waters. On the other hand, with respect to the other studied sites, the absence at Campo

447   Pisano of a vegetation cover limiting wind and water erosion makes this site a potential centre of

448   mechanical dispersion of contaminants.

449   Considering the potential mobilization to the biosphere, Concas (2014) showed that Pb is much less

450   mobile than Zn with respect to uptake by *P. lentiscus*. This limited Pb uptake was ascribed to a

451   combination of the lower Pb mobility, and of a physiological mechanism of exclusion (Zn is an

452   essential micronutrient, whereas Pb has no known physiological function, and may have phytotoxic

453   effects – Shahid et al., 2012). Concas (2014) also showed that Pb and Zn uptake of *P. lentiscus*

454   varies seasonally. Since field pore water and plant sampling did not occur at the same time (plants

455   were sampled in May and September 2012), it is not possible to compare directly plant uptake and

456   metal concentration of the pore water. Moreover, plant uptake is clearly influenced also by the total

457   amount of available pore water, and not only by metal concentrations. This aspect could well be

458   worthy a future step of investigation. The authors notice here that this kind of information could be

459   useful for the management of a mining waste dump subjected to phytostabilization. For example, a

460   water-saving watering system could be planned in specific periods of the year in order to modify

461   pore water composition, to obtain a decrease of some element when necessary. As a consequence of

462   Zn mobilization to the biosphere, there is a potential risk that this metal could enter the trophic

463   chain. On the other hand, phytostabilization actions using *P. lentiscus* as a pioneer species should

464   not be impaired, inasmuch as this species is well tolerant to Zn (Bacchetta et al., 2012; Concas,

465   2014).

466

467   **5. Conclusions**

468

469   Field sampling and chemical monitoring of soil pore water in the major abandoned mining district

470   of Iglesiente (SW Sardinia) confirmed that pore water is a rapid and easy method to collect reliable

471   information on the potential risk of a contaminated soil.

472   Soil pore waters chemistry in the studied sites reflects the mineralogy of the local soil, and suggests

473   an approach to equilibrium with coexisting solid phases. This aspect permits to easily evaluate

474   which minerals are likely responsible for controlling (toxic) element mobility.

475   With respect to laboratory tests on metal mobility, the analysis of pore water permits to evaluate

476   trace elements mobility, and the consequent environmental risk, also following pore water seasonal

477   changes both in qualitative and quantitative terms. Pore water represents the most available fraction

478   of the overall soil matrix for plant uptake, therefore allowing a direct comparison with possible

479   seasonal changes in metal uptake by plants. In fact, in a companion study of the local species *P.*

480   *lentiscus*, local and seasonal variations of metal (Zn, Pb and Hg) concentrations in different parts of

481   the plant were detected. Such variations may be partially a response to local/seasonal changes of

482   pore water quantitative/qualitative characteristics. This kind of information could be useful for the

483   management of a mining waste dump interested by phytostabilization.

484

490

References

Ardau, C., Blowes, D.W., Ptacek, C.J., 2009. Comparison of laboratory testing protocols to field observations of the weathering of sulfide-bearing mine tailings. J Geochem Explor 100,182–191.

Ardau, C., Podda, F., Da Pelo, S., Frau, F., 2013. Stream water chemistry in the arsenic-contaminated Baccu Locci mine watershed (Sardinia, Italy) after remediation. Environ Sci Pollut Res 7550–7559.

Ardau, C., Lattanzi, P., Peretti, R., Zucca, A., 2014. Chemical stabilization of metals in mine wastes by transformed red mud and other iron compounds: laboratory tests. Environm Technol 35 (24), 3060–3073.

Aru, A., Madeddu, B., Kahnamoei, A., 1995. Soil contamination by heavy metals from mines. In Land use and soil degradation – MEDALUS in Sardinia. Aru A., Enne G., Pulina G. (eds.). La Celere Editrice: Alghero, Italy, 265–283.

Bacchetta, G., Cao, A., Cappai, G., Carucci, A., Casti, M., Fercia, M.L., Lonis, R., Mola, F., 2012. A field experiment on the use of *Pistacia lentiscus* L. and *Scrophularia canina* L. subsp. bicolor (Sibth. et Sm.) Greuter for the phytoremediation of abandoned mining areas. Plant Biosyst 146, 1054–1063.

Back, W., 1966. Hydrochemical facies and ground-water flow patterns in northern part of Atlantic Coastal Plain. U.S. Geol Surv Professional Paper 498–A.

Barbafieri, M., Dadea, C., Tassi, E., Bretzel, F., Fanfani, L., 2011. Uptake of Heavy Metals by Native Species Growing in a Mining Area in Sardinia, Italy: Discovering Native Flora for Phytoremediation. Int J Phytoremediat 13 (10), 985–997.

Bechstädt, T., Boni, M., 1994 (Eds.). Sedimentological, stratigraphical and ore deposits field guide of the autochthonous Cambro–Ordovician of southwestern Sardinia. Memorie Descrittive della Carta Geologica d'Italia, Servizio Geologico Nazionale 48,155–184.

Beesley, L., Moreno-Jiménez, E., Clemente, R., Lepp, N., Dickinson, N., 2010. Mobility of arsenic, cadmium and zinc in a multi-element contaminated soil profile assessed by in-situ soil pore water sampling, column leaching and sequential extraction. Environ Pollut 158, 155–160.

Blowes, D.W., Ptacek, C.J., Jambor, J.L., Weisener, C.G., 2003. The geochemistry of acid mine drainage, In: Lollar, B.S. (Ed.), Environ Geochem vol. 9 Treatise on Geochemistry (eds. Holland, H.D.; Turekian, K.K.), Vol. 9, Elsevier-Pergamon, Oxford, 149–204.

Boni, M., Costabile, S., De Vivo, B., Gasparrini, M., 1999. Potential environmental hazard in the mining district of southern Iglesiente (SW Sardinia, Italy). J Geochem Explor 67, 417–430.

525 Boni, M., Gilg, H.A., Aversa, G., Balassone, G., 2003. The "Calamine" of Southwest Sardinia:
526   Geology, Mineralogy, and Stable Isotope Geochemistry of Supergene Zn Mineralization.
527   Econ Geol 98, 731–748.

528 Brunori, C., Cremisini, C., D'Annibale, L., Massanisso, P., Pinto, V., 2005. A kinetic study of trace
529   element leachability from abandoned mine-polluted soil treated with SS-MSW compost and
530   red mud. Comparison with results from sequential extraction. Anal Bioanal Chem 381, 1347–
531   1354.

532 Cao, A., Carucci, A, Lai, T., La Colla, P., Tamburini, E., 2007. Effect of biodegradable chelating
533   agents on heavy metals phytoextraction with *Mirabilis jalapa* and on its associated bacteria.
534   Eur J Soil Biol 43, 200–206.

535 Cao, A., Carucci, A., Lai, T., Bacchetta, G., Casti, M., 2009. Use of native species and
536   biodegradable chelating agents in the phytoremediation of abandoned mining areas. J Chem
537   Technol Biotechnol 84, 884–889.

538 Chaney, R.L., Malik, M., Li, Y.M., Brown, S.L., Angle, J.S., Baker, A.J.M., 1997.
539   Phytoremediation of soil metals. Curr Opin Biotech 8, 279-284.

540 Cidu, R., Biagini, C., Fanfani, L., La Ruffa, G., Marras, I., 2001. Mine closure at Monteponi (Italy):
541   Effect of the cessation of dewatering on the quality of shallow groundwater. Appl Geochem
542   16, 489–502.

543 Cidu, R. , Frau, F., Da Pelo, S., 2011. Drainage at Abandoned Mine Sites: Natural Attenuation of
544   Contaminants in Different Seasons. Mine Water Environ 30, 113–126.

545 Cidu, R., Dadea, C., Desogus, P., Fanfani, L., Manca, P.P., Orrù, G., 2012. Assessment of
546   environmental hazards at abandoned mining sites: A case study in Sardinia, Italy. Appl
547   Geochem 27, 1795–1806.

548 Concas, A., Ardau, C., Cristini, A., Zuddas, P., Cao, G., 2006. Mobility of heavy metals from
549   tailings to stream waters in a mining activity contaminated site. Chemosphere 63, 244–253.

550 Concas, S., 2014. Studio delle forme chimiche e mineralogiche e della mobilità/biodisponibilità di
551   metalli pesanti in suoli, piante (*Pistacia lentiscus* L.) e soluzioni del suolo del Bacino del Rio
552   San Giorgio (Iglesias − Gonnesa, Sardegna sud - occidentale, Italia) finalizzato allo sviluppo
553   di strategie di soil remediation. Ph.D. Thesis, Università di Cagliari (partly in Italian).
554   http://veprints.unica.it/943/

555 Concas, S., Lattanzi, P., Bacchetta, G., Barbafieri, M., Vacca, A., (submitted) Zn, Pb and Hg
556   contents of *Pistacia lentiscus* L. grown on heavy-metal rich soils: implications for
557   phytostabilization. Water Air Soil Poll.

558 Cui, J., Zang, S., Zhai, D., Wu, B., 2014. Potential ecological risk of heavy metals and metalloid in
559   the sediments of Wuyuer River basin, Heilongjiang Province, China. Ecotoxicology 23 (4),
560   589–600.

561 De Siervi, M., Iorio, A.F., Chagas, C.I., 2004. Concentración total de Ni, Cr, Pb y Cd en suelos de
562   la Cuenca del Arroyo Morales, Buenos Aires. XIX Congreso Argentino de la Ciencia del
563   Suelo, Paraná, EntreRios, en CD, 10pp.

564 Di Bonito, M., Breward, N., Crout, N., Smith, B., Young, S., 2008. Overview of Selected Soil Pore
565   Water Extraction Methods for the Determination of Potentially Toxic Elements in
566   Contaminated Soils: Operational and Technical Aspects. Environmental Geochemistry. Site
567   Characterization, Data Analysis and Case Histories, 213–249.

568 Fanfani, L., Ardau, C., 2011. A worldwide emergency: arsenic risk in water. Case study of an
569   abandoned mine in Italy - In: "Water Security in the Mediterranean Region - An International
570   Evaluation of Management, Control, and Governance Approaches" Publisher "Springer",
571   Editors B. El Mansouri & A. Scozzari, series "NATO Science for Peace and Security Series
572   C", pp 177–190.

573 Franzini M., Leoni L., 1972. A full matrix correction in X-Ray fluorescence analysis of rock
574   samples. Atti Soc. Toscana Sci. Nat., Mem., Serie A 79, 7–22.

575 González, R.C., González-Chávez, M.C.A., 2006. Metal accumulation in wild plants surrounding
576   mining wastes. Environ Pollut 144, 84–92.

577 Impelliteri, C.A., Saxe, J.K., Cochran, M., Janssen, G., Allen, H.E., 2003. Predicting the
578   bioavailability of copper and zinc in soils: Modeling the portioning of potentially bioavailable
579   copper and zinc from soil solid to soil solution. Environ Toxicol Chem 22, 1380–1386.

580 IUSS Working Group WRB, 2014. World Reference Base for Soil Resources 2014. International
581   soil classification system for naming soils and creating legends for soil maps. World Soil
582   Resources Reports No. 106. FAO, Rome.

583 Lekakis, E., Aschonitis, V., Pavlatou-Ve, A., Papadopoulos, A., Antonopoulos, V., 2015. Analysis
584   of Temporal Variation of Soil Salinity during the Growing Season in a Flooded Rice Field of
585   Thessaloniki Plain-Greece. Agronomy 5 (1), 35–54.

586 Li, M., Zang, S., Xiao, H., Wu, C., 2014. Speciation and distribution characteristics of heavy metals
587   and pollution assessments in the sediments of Nashina Lake, Heilongjiang, China.
588   Ecotoxicology 23 (4), 681–688.

589 Lomelin, G.J., 2002. Informe anual ambiental. Peñoles, México. [On line]. Available from
590   <http://www.economia-dgm.gob.mx/informe/index.html>.

591 Lorrai, M., Fanfani, L., 2007. Effect of sea spray on the chemistry of granitoid aquifers in coastal
592   areas. Water-Rock Interaction - Proceedings of the 12th International Symposium on Water-
593   Rock Interaction, WRI-12.

594 Marescotti, P., Carbone, C., Comodi, P., Frondini, F., Lucchetti, G., 2012. Mineralogical and
595   chemical evolution of ochreous precipitates from the Libiola Fe–Cu-sulfide mine (Eastern
596   Liguria, Italy). Appl Geochem 27, 577–589.

597 Meers, E., Du Laing, G., Unamuno, V., Ruttens, A., Vangronsveld, J., Tack, F.M.G., Verloo, M.G.,
598   2007. Comparison of cadmium extractability from soils by commonly used single extraction
599   protocols. Geoderma 141, 247–259.

600 Mendez, M.O., Maier R. M., 2008. Phytostabilization of Mine Tailings in Arid and Semiarid
601   Environments—An Emerging Remediation Technology. Environ Health Perspect 116 (3),
602   278–283.

603 Ministero delle Politiche Agricole e Forestali (MiPAF), 1998. Metodi di analisi fisica del suolo.
604   Collana di metodi analitici per l'agricoltura. Franco Angeli Editore, Milano, Italy.

605 Ministero delle Politiche Agricole e Forestali (MiPAF), 2000. Metodi di analisi chimica del suolo
606   (in Italian). Collana di metodi analitici per l'agricoltura, Franco Angeli Editore, Milano, Italy.

607 Moreno-Jiménez, E., Beesley, L., Lepp, N.W., Dickinson, N.M., Hartley,W., Clemente, R., 2011.
608   Field sampling of soil pore water to evaluate trace element mobility and associated
609   environmental risk. Environ Pollut 159, 3078–3085.

610 Nkongolo, K.K., Spiers, G., Beckett, P., Narendrula, R., Theriault, G., Tran, A., Kalubi, K.N., 2013.
611   Long-term effects of liming on soil chemistry in stable and eroded upland areas in a mining
612   region. Water Air Soil Poll 224: 1618, 14pp

613 Nicoară, A., Neagoe, A., Stancu, P., De Giudici, G., Langella, F., Sprocati, A.R., Iordache, V.,
614   Kothe, E., 2014. Coupled pot and lysimeter experiments assessing plant performance in
615   microbially assisted phytoremediation. Environ Sci Pollut Res 21, 6905–6920.

616 Parkhurst, D.L., Thorstenson, D.C., Plummer, L.N., 1980. PHREEQE--A computer program for
617   geochemical calculations. U.S. Geological Survey Water-Resources Investigations Report 80,
618   96–195.

619 Parkhurst, D.L., 1995. User's guide to PHREEQC--A computer program for speciation, reaction-
620   path, advective-transport, and inverse geochemical calculations. U.S. Geological Survey
621   Water-Resources Investigations Report 95, 4227, 143.

622 RAS, 2003. Piano regionale di gestione dei rifiuti. Piano di bonifica siti inquinati. Regione
623   Autonoma della Sardegna (in Italian).

RAS, 2010. Prima predisposizione del piano di gestione del distretto idrografico. Regione Autonoma della Sardegna (in Italian).

Schoeneberger, P.J., Wysocki, D.A., Benham, E.C., Broderson, W.D. (Eds.), 2002. Field Book for Describing and Sampling Soils, Version 2.0. Natural Resources Conservation Service, National Soil Survey Center: Lincoln, NE.

Shaheen, S.M., Rinklebe, J., Rupp, H., Meissner, R., 2014. Temporal dynamics of pore water concentrations of Cd, Co, Cu, Ni, and Zn and their controlling factors in a contaminated floodplain soil assessed by undisturbed groundwater lysimeters. Environ Pollut 191, 223–231.

Shahid, M., Pinelli, E., Dumat, C., 2012. Review of Pb availability and toxicity to plants in relation with metal speciation; role of synthetic and natural organic ligands. J Hazard Mater 219– 220, 1–12.

Shahid, M., Pinelli, E., Pourrut, B., Dumat, C., 2014. Effect of organic ligands on lead-induced oxidative damage and enhanced antioxidant defense in the leaves of *Vicia faba* plants. J Geochem Explor 144, 282–289.

Sneddon, I.R., Orueetxebarria, M., Hodson, M., Schofield, P.F., Valsami-Jones, E., 2006. Use of bone-meal amendments to immobilize Pb, Zn and Cd in soil: a leaching column study. Environ Pollut 144, 816–825.

Tipping, E., 1994. WHAM — A chemical equilibrium model and computer code for waters, sediments and soils incorporating a discrete-site/electrostatic model of ion-binding by humic substances. Comput Geosci-UK 20, 973–1023.

Tye, A.M., Young, S.D., Crout, N.M.J., Zhang, H., Preston, S., Barbosa-Jefferson, V.L., Davison, W., McGrath, S.P., Paton, G.I., Kilham, K., Resende, L., 2003. Predicting the activity of Cd^{2+} and Zn^{2+} in soil pore water from the radio-labile metal fraction. Geochim Cosmochim Acta 67, 375–385.

Vacca, A., Vacca, S., 2001. Soil degradation in Sardinia – Historical causes and current processes due to anthropogenic pressure. Petermann Geogr Mitt 145, 68–78.

Vacca, A., Bianco, M.R., Murolo, M., Violante, P., 2012. Heavy metals in contaminated soils of the Rio Sitzerri flood plain (Sardinia, Italy): characterization and impact on pedodiversity. Land Degrad Dev 23, 350–364.

Vázquez, S., Moreno, E., Carpena, R.O., 2008. Bioavailability of metals and As from acidified multi contaminated soils: use of white lupin to validate several extraction methods. Environ Geochem Hlth 30, 193–198.

Vig, K., Megharaj, M., Sethunathan, N., Naidu, R., 2003. Bioavailability and toxicity of cadmium to microorganisms and their activities in soil: A review. Adv Environ Res 8, 121–135.

658   Whipkey, C.E., Capo, R.C., Chadwick, O.A., Stewart, B.W., 2000. The contribution of sea spray
659   aerosol to the soil cation budget in a Hawaiian coastal environment. Chem. Geol. 168: 37–48
660

661   **Table captions**

662

663   Table 1. Selected soil properties at the sampling sites

664

665   Table 2a and 2b. Major and selected trace element analysis of soils at the sampling sites,

666   distinguished for horizons

667

668   Table 3a and 3b. Pore water parameters (T°, pH, conductivity) and major chemistry distinguished

669   for sampling site, sampling time, and sampling method.

670

671   Table 4a and 4b. Selected trace elements in pore waters distinguished for sampling site, sampling

672   time, and sampling method. Bold font indicates values above limits established by Italian laws

673   (D.lgs 152/2006) for subsurface waters.

674

675   Table 5. Main element speciation in pore waters as determined by PHREEQC and WHAM codes.

676 **Figure captions**

677

678 Figure 1. Schematic map of the study area, with location of sampling points.

679

680 Fig. 2. a) general view of the Campo Pisano experimental plots established in 2008 by Bacchetta et

681 al. (2012), pointing those selected for this study; b) and c) vertical sections of 'soils' in Plot 1 and

682 Plot 3; in the first (untreated material) *P. lentiscus* planted in 2008 did not survive, whereas several

683 individuals survived in Plot 3, where compost was added as amendment.

684

685 Fig. 3. Piper diagram illustrating the variability in major ion composition of the studied pore waters.

686

687 Fig. 4. Saturation indexes for selected minerals, distinct for sampling site (symbol), and ordered for

688 sampling time (from right to left). The solid line (SI = 0) indicates equilibrium between mineral and

689 solution. See text for the assessment of the role of selected minerals from (a) to (h) in controlling

690 element mobility in pore waters.

691

692 Fig. 5. Na vs Cl plot of pore water samples from Sa Masa site (P9). The linear trend suggests a co-

693 variation of the two elements due to seasonal variations.

Table 1

Soil	Horizon	Depth	Texture			Textural class[a]	pH (H$_2$O)	OC
			Sand	Silt	Clay			
		cm		%				g kg^{-1}
P1	^ACm	0–0.3/0.5	77.7	20.9	1.4	ls	7.6	11
	^AC1	0.3/0.5–8/14	82.5	16.7	0.8	ls	7.5	9
	^AC2	8/14–16.5/20.5	69.6	29.3	1.1	sl	7.3	14
	2^C	16.5/20.5–>30	68.4	28.3	3.3	sl	4.5	2
P3	^Ap1	0–1.5/1.8	73.8	24.8	1.4	ls	7.2	61
	^Ap2	1.5/1.8–15/17	77.9	21.3	0.8	ls	7.1	66
	2^C	15/17–>22	66.8	31.1	2.1	sl	4.8	5
P5	A	0–15	44.1	41.6	14.3	l	7.3	43
	AB	15–28	30.7	39.9	29.4	cl	7.3	27
	Bw	28–60/65	13.6	26.6	59.8	c	7.3	11
	R	>60/65						
P6	A	0–10	44.1	43.8	12.1	l	7.1	37
	Bw	10–37/50	31.5	41.2	27.3	cl	7.5	18
	R	>37/50						
P9	A	0–8	47.2	49.8	3.0	l	7.5	25
	2C1	8–12	18.4	76.2	5.4	sil	7.8	9
	3C2	12–25	73.6	24.6	1.8	ls	7.8	6
	4C3	25–40	53.0	45.9	1.1	sl	7.8	5
	5C4	40–59	34.1	63.6	2.3	sil	8.0	6
	6C5	59–>120	86.9	12.1	1.0	ls	8.1	5

[a] ls = loamy sand; sl = sandy loam; l = loam; cl = clay loam; c = clay; sil = silt loam.

Soil	Horizon	Depth (cm)	LOI	Na_2O	MgO	Al2O$_3$	SiO_2	P_2O_5	K_2O	CaO	TiO_2	MnO	Fe_2O_3	Other*	Tot
		(cm)	%	%	%	%	%	%	%	%	%	%	%	%	%
P1	^ACm	0-0.3/0.5	28.84	0.40	13.9	3.81	14.3	0.04	0.59	23.2	0.13	0.24	13.5	1.52	100
	^AC1	0.3/0.5-8/14	26.69	0.33	13.5	4.13	14.5	0.04	0.60	25.0	0.12	0.25	10.7	1.47	97.0
	^AC2	8/14-16.5/20.5	24.25	0.61	15.2	2.84	11.9	0.04	0.53	26.0	0.13	0.23	17.0	1.69	100
	2^C	16.5/20.5->30	13.70	0.25	0.50	2.57	9.21	0.03	0.49	23.9	0.12	0.02	48.5	0.79	100
P3	^Ap1	0-1.5/1.8	25.32	0.41	5.43	5.71	21.9	0.89	0.93	20.6	0.16	0.20	17.6	1.12	100
	^Ap2	1.5/1.8-15/17	24.71	0.52	9.46	4.28	18.9	0.25	0.82	23.2	0.16	0.17	16.8	1.00	100
	^2C	15/17- >22	12.75	0.11	0.18	2.25	7.67	0.05	0.40	25.8	0.09	0.02	50.2	0.65	100
P5	A	0-15	12.56	0.23	1.19	20.8	52.1	0.15	1.92	0.62	0.44	0.49	8.15	1.55	100
	Ab	15-28	10.65	0.25	1.41	21.3	50.9	0.13	2.27	0.47	0.53	0.51	9.79	1.94	100
	Bw	28-60/65	10.50	0.22	1.32	26.9	44.7	0.08	2.59	0.34	0.45	0.40	11.7	0.90	100
P6	A	0-10	11.43	0.60	1.96	16.9	54.0	0.15	2.84	0.95	0.81	0.96	8.91	0.61	100
	Bw	10-37/50	8.51	0.49	1.80	21.2	52.8	0.12	2.79	0.60	0.76	0.87	9.38	0.68	100
P9	2C1	8-12	28.89	0.65	5.33	3.28	23.1	0.04	0.39	32.4	0.17	0.18	3.68	2.69	100
	3C2	12-25	31.68	0.48	6.61	2.48	18.2	0.03	0.25	35.7	0.17	0.22	2.71	2.23	100
	4C3	25-40	33.48	0.41	6.61	1.17	14.4	0.02	0.19	40.1	0.09	0.22	2.23	1.73	100
	5C4	40-59	35.37	0.46	7.99	1.30	10.5	0.02	0.19	38.7	0.09	0.24	3.89	1.96	100
	6C5	59- >120	31.77	0.62	8.22	1.31	10.3	0.02	0.21	35.2	0.09	0.20	9.24	4.13	100

° Except the A horizon at the P9 location – see text

*Sum of elements in Table 2b

Table 2a

Profile	Horizon	Depth (cm)	Cd	Cu	Ni	Pb	Zn
					mg/kg		
	^ACm	0-0.3/0.5	70	52	< 16	2180	12932
P1	^AC1	0.3/0.5-8/14	72	44	< 16	2180	12402
	^AC2	8/14-16.5/20.5	78	92	< 16	2126	14646
	2^C	16.5/20.5- >30	15	56	< 16	2698	5119
	^Ap1	0-1.5/1.8	54	54	< 16	1760	9360
P3	^Ap2	1.5/1.8-15/17	54	51	< 16	1566	8327
	^2C	15/17- >22	16	57	< 16	2776	3666
	A	0-15	6	56	39	13642	1779
P5	Ab	15-28	<4	54	39	17697	1655
	Bw	28-60/65	<4	56	53	7134	1822
	R	60/65- >60/65	10	10	< 16	1754	426
	A	0-10	30	37	41	1360	4680
P6	Bw	10-37/50	30	31	44	1453	5244
	R	37/50- >37/50	<4	<8	< 16	<d.l.	1097
	A	0-8	265	330	< 16	37616	220946
	2C1	8-12	153	72	< 16	4300	22400
P9	3C2	12-25	89	49	< 16	3401	18805
	4C3	25-40	70	45	< 16	3398	13792
	5C4	40-59	92	45	< 16	2335	17122
	6C5	59- >120	146	83	< 16	5927	35173

Table 2b

Site	sample	t (°C)				pH				λ (µS cm^{-1})				alkalinity (mg L^{-1})				Organic Carbon (mg L^{-1})			
		Dec	Jan	Febr	Apr	Dec	Jan	Febr	Apr	Dec	Jan	Febr	Apr	Dec	Jan	Febr	Apr	Dec	Jan	Febr	Apr
P1	1	14.5	11.2	14.5	-	9.21	8.26	7.15	-	-	1818	2060	-	18	-	57	-	11.4	<0.04	3.3	-
P3	2	17.2	10.9	15.5	-	8.73	8.51	7.38	-	-	1240	2020	-	44	89	147	-	12.6	7.1	10.7	-
P9 long lysimeter	4a	13.9	11.2	13	-	8.12	7.39	7.31	-	-	2630	2770	-	69	180	307	-	6.48	1.9	1.8	-
	4b	13.7	11.3	12.2	-	7.91	7.41	7.11	-	-	3750	2840	-	47	158	314	-	6.93	2.3	2.1	-
	4c	13.7	10.8	11.3	-	7.72	7.03	7.26	-	-	3240	2740	-	111	167	307	-	3.25	1.6	1.6	-
P9 short lysimeter	5a	13.7	10.7	12.6	-	8.31	7.88	7.55	-	-	2900	2450	-	55	114	237	-	8.1	<0.04	2.9	-
	5b	-	10.6	12.3	-	-	7.64	7.39	-	-	2600	2420	-	-	136	245	-	-	1.2	4.8	-
P9 rizhometer	19	-	-	-	24	-	-	-	7.93	-	-	-	2440	-	-	-	151	-	-	-	5.1
P9 rizhometer	22	-	-	-	16.8	-	-	-	7.78	-	-	-	2180	-	-	-	152	-	-	-	5.62
P9 rizhometer	25	-	-	-	20	-	-	-	7.62	-	-	-	2460	-	-	-	154	-	-	-	3.97
P9 short lysimeter	25	-	-	-	18.7	-	-	-	7.5	-	-	-	2620	-	-	-	192	-	-	-	4.79
P5	6a	-	-	15.2	-	-	-	8.87	-	-	-	566	-	-	-	243	-	-	-	3.3	-
	6b	-	11.8*	14.3	-	-	9.14*	8.87	-	-	577*	706	-	-	178*	275	-	-	4.3*	4.1	-
	6c	-	11.8*	15.9	-	-	9.14*	8.8	-	-	577*	696	-	-	178*	252	-	-	4.3*	3.8	-
P6	7a	-	-	14.2	-	-	-	8.9	-	-	-	797	-	-	-	278	-	-	-	4.0	-
	7b	-	11.4	14.8	-	-	9.16	9.02	-	-	910	961	-	-	210	339	-	-	<0.04	4.7	-
	7c	-	-	12.5	-	-	-	9.05	-	-	-	679	-	-	-	401	-	-	-	2.4	-

* = 6b + 6c average; - = not analysed

Table 3a

Site	sample	Cl (mg L⁻¹)				SO⁴ (mg L⁻¹)				Ca²⁺ (mg L⁻¹)				Mg²⁺ (mg L⁻¹)				Na⁺ (mg L⁻¹)				K⁺ (mg L⁻¹)			
		Dec	Jan	Feb	Apr	Dec	Jan	Feb	Apr	Dec	Jan	Feb	Apr	Dec	Jan	Feb	Apr	Dec	Jan	Feb	Apr	Dec	Jan	Feb	Apr
P1	1	30	16	24	-	855	1480	1290	-	316	460	469	-	34	98	54	-	18	11	14	-	1	1	0.0	-
P3	2	14	43	10	-	783	1044	1082	-	314	393	468	-	39	62	45	-	7	22	9	-	2	6	0.9	-
P9 long lysimeter	4a	443	368	272	-	1385	1186	962	-	433	322	279	-	156	132	105	-	326	268	205	-	26	21	17	-
	4b	448	437	279	-	1429	1404	1070	-	438	376	294	-	161	157	106	-	332	310	205	-	27	24	18	-
	4c	439	357	270	-	1382	1184	978	-	422	332	275	-	148	122	100	-	319	262	198	-	24	21	18	-
P9 short lysimeter	5a	398	337	255	-	1252	1187	920	-	338	295	259	-	135	133	103	-	285	255	194	-	21	21	16	-
	5b	-	346	258	-	-	1186	924	-	-	326	271	-	-	119	98	-	-	253	197	-	-	21	17	-
P9 rizhometer	19	-	-	-	274	-	-	-	757	-	-	-	219	-	-	-	75	-	-	-	168	-	-	-	16
P9 rizhometer	22	-	-	-	260	-	-	-	893	-	-	-	262	-	-	-	83	-	-	-	184	-	-	-	16
P9 rizhometer	25	-	-	-	302	-	-	-	753	-	-	-	286	-	-	-	78	-	-	-	178	-	-	-	17
P9 short lysimeter	25	-	-	-	256	-	-	-	919	-	-	-	259	-	-	-	91	-	-	-	187	-	-	-	17
P5	6a	-	-	23		-	-	7		-	-	36		-	-	36	-	-	-	26	-	-	-	10	-
	6b	-	31*	30		-	6*	4		-	23*	23		-	41*	67	-	-	23*	34	-	-	9*	11	-
	6c	-	31*	18		-	6*	15		-	23*	42		-	41*	55	-	-	23*	26	-	-	9*	9.9	-
P6	7a	-	-	64		-	-	14		-	-	36		-	-	66	-	-	-	33	-	-	-	6.2	-
	7b	-	168	123		-	14	16		-	27	31		-	120	69	-	-	68	62	-	-	28	25	-
	7c	-	-	40		-	-	13		-	-	0		-	-	54	-	-	-	43	-	-	-	6.7	-

*= 6 b + 6c average; - = not analysed

Table 3b

Site	sample	Zn µg L^{-1}				Pb µg L^{-1}				Cd µg L^{-1}			
		Dec	Jan	Febr	Apr	Dec	Jan	Febr	Apr	Dec	Jan	Febr	Apr
P1	1	20	126	172	-	**22**	**17**	**18**	-	-	<0.4	2.3	-
P3	2	38	145	206	-	**36**	**18**	**32**	-	-	<0.4	3.6	-
P9 long lysimeter	4a	127	**6226**	**4324**	-	21	30	<5	-	-	<0.4	1.4	-
	4b	117	**6261**	**4613**	-	12	28	<5	-	-	<0.4	2.3	-
	4c	481	**7861**	**5666**	-	20	23	14	-	-	<0.4	3.7	-
P9 short lysimeter	5a	60	1497	1516	-	16	23	18	-	-	<0.4	2.5	-
	5b	-	2530	**3195**	-	-	19	23	-	-	<0.4	**7.1**	-
P9 rizhometer	19	-	-	-	1665	-	-	-	**64**	-	-	-	5
P9 rizhometer	22	-	-	-	2056	-	-	-	10	-	-	-	**7**
P9 rizhometer	25	-	-	-	2274	-	-	-	**18**	-	-	-	**10**
P9 short lysimeter	25	-	-	-	1597	-	-	-	<5	-	-	-	3
P5	6a	-	-	35	-	-	-	<5	-	-	-	<1.3	-
	6b	-	31*	41	-	-	**64***	**18.6**	-	-	<0.4*	<1.3	-
	6c	-	31*	127	-	-	**64***	<5	-	-	<0.4*	<1.3	-
P6	7a	-	-	23	-	-	-	<5	-	-	-	<1.3	-
	7b	-	24	30	-	-	**46**	<5	-	-	<0.4	<1.3	-
	7c	-	-	18	-	-	-	**13**	-	-	-	<1.3	-

*= b + c average; - = not analysed

Table 4a

Site	sample	Mn µg L^{-1}				Fe µg L^{-1}				Cu µg L^{-1}			
		Dec	Jan	Febr	Apr	Dec	Jan	Febr	Apr	Dec	Jan	Febr	Apr
P1	1	9	10	<0.01	**117**	0.4	13	119	-	8.0	<0.5	<1.2	-
P3	2	16	13	<0.01	**200**	98	19	<5.3	-	26	4.8	2	-
P9 long lysimeter	4a	**140**	**226**	**141**	**74**	47	11	7	-	4.9	5.9	11	-
	4b	**68**	**230**	**62**	**73**	<0.1	13	<5.3	-	4.6	1.9	3	-
	4c	**63**	**92**	5	**70**	<0.1	6.0	<5.3	-	2.2	1.7	2	-
P9 short lysimeter	5a	15	**59**	3	**77**	15	2.2	<5.3	-	6.0	4.6	8.9	-
	5b	-	22	<0.01	-	-	15	<5.3	-	-	0.7	4	-
P9 rizhometer	19	-	-	-	<0.01	-	-	-	-	-	-	-	<1.2
P9 rizhometer	22	-	-	-	<0.01	-	-	-	-	-	-	-	<1.2
P9 rizhometer	25	-	-	-	<0.01	-	-	-	-	-	-	-	4
P9 short lysimeter	25	-	-	-	<0.01	-	-	-	-	-	-	-	2
	6a	-	-	-	-	-	-	-	-	-	-	-	-
P5	6b	-	9*	-	-	-	23*	<5.3	-	-	7*	4.3	-
	6c	-	9*	-	-	-	23*	<5.3	-	-	7*	<1.2	-
	7a	-	-	-	-	-	-	<5.3	-	-	-	<1.2	-
P6	7b	-	9	-	-	-	24	<5.3	-	-	8	<1.2	-
	7c	-	-	-	-	-	-	<5.3	-	-	-	<1.2	-

*= b + c average; - = not analysed

Table 4b

Site	sampler	Species* (PHREEQC)	fraction bound to colloidal FA (WHAM)
P1	1 - Dec	Ca^{2+}, $CaSO_4$, $CuOH^+$, Mg^{2+}, $MgSO_4$, Mn^{2+}, $MnSO_4$, $PbOH^+$, $PbCO_3$, Pb^{2+}, Zn^{2+}, $ZnSO_4$	Cu (80%), Zn (3.5%), Pb (0.2%)
	1 - Jan	Ca^{2+}, $CaSO_4$, Mg^{2+}, $MgSO_4$, Mn^{2+}, $MnSO_4$, $PbOH^+$, $PbCO_3$, Pb^{2+}, Zn^{2+}, $ZnSO_4$	no O.C.
	1 - Febr	Ca^{2+}, $CaSO_4$, Mg^{2+}, $MgSO_4$, Pb^{2+}, $PbCO_3$, Zn^{2+}, $ZnSO_4$	Zn (2.4%), Cd (1.15%), Pb (0.015%)
P3	2 - Dec	Ca^{2+}, $CaSO_4$, $CuCO_3$, Mn^{2+}, $MnSO_4$, $PbCO_3$, Zn^{2+}, $ZnSO_4$	Cu (60%), Zn (5%), Pb (0.1%)
	2 - Jan	Ca^{2+}, $CaSO_4$, $CuOH^+$, $CuCO_3$, Mg^{2+}, $MgSO_4$, Mn^{2+}, $MnSO_4$, $MnCO_3$, $PbCO_3$, $PbOH^+$, Zn^{2+}, $ZnSO_4$	Cu (55%), Zn (3.2%), Pb (0.06%)
	2 - Febr	Ca^{2+}, $CaSO_4$, $CuCO_3$, Mg^{2+}, $MgSO_4$, $PbCO_3$, Zn^{2+}, $ZnSO_4$	Cu (99%), Zn (8.8%), Cd (3.6%), Pb (70%)
P5	6b+c - Jan	Ca^{2+}, $CaSO_4$, $CuCO_3$, $Cu(CO_3)_2^{2-}$, Mg^{2+}, $MgSO_4$, $MnCO_3$, Mn^{2+}, $PbCO_3$, $Pb(CO_3)_2^{2-}$ $PbOH^+$, $Zn(OH)_2$, Zn^{2+}, $ZnCO_3$	Cu (39%), Zn (3.5%)
	6a - Febr	Ca^{2+}, $CaCO_3$, Mg^{2+}, $MgCO_3$, $Zn(OH)_2$, Zn2+, $ZnCO_3$	Zn (4.8%)
	6b - Febr	Ca^{2+}, $CaCO_3$, $CuCO_3$, $Cu(CO_3)_2^{2-}$, Mg^{2+}, $MgCO_3$, $PbCO_3$, $Pb(CO_3)_2^{2-}$, Zn^{2+}, $ZnCO_3$	Cu (60%), Zn (3%), Pb (0.9%)
	6c - Febr	Ca^{2+}, $CaCO_3$, Mg^{2+}, $MgCO_3$, $Zn(OH)_2$, Zn^{2+}, $ZnCO_3$	Zn (3%)
P6	7b - Jan	Ca^{2+}, $CuCO_3$, $Cu(CO_3)_2^{2-}$, Mg^{2+}, $MgCO_3$, $MnCO_3$, Mn^{2+}, $PbCO_3$, $Pb(CO_3)_2^{2-}$, $PbOH^+$, $Zn(OH)_2$, Zn^{2+}, $ZnCO_3$	no O.C.
	7a Febr	Ca^{2+}, $CaCO_3$, Mg^{2+}, $MgCO_3$, $Zn(OH)_2$, Zn^{2+}, $ZnCO_3$	Zn (5%)
	7b - Febr	Ca^{2+}, $CaCO_3$, Mg^{2+}, $MgCO_3$, $Zn(OH)_2$, Zn^{2+}, $ZnCO_3$	Zn (5.5%)
	7c - Febr	Ca^{2+}, $CaCO_3$, Mg^{2+}, $MgCO_3$, $PbCO_3$, $Pb(CO_3)_2^{2-}$, $Zn(OH)_2$, Zn^{2+}, $ZnCO_3$	Zn (5%), Pb (1%)
P9 long lysimeter	4a - Dec	Ca^{2+}, $CaSO_4$, $CuCO_3$, Mg^{2+}, $MgSO_4$, Mn^{2+}, $MnSO_4$, $PbCO_3$, Zn^{2+}, $ZnSO_4$	Cu (20%), Zn (1%)
	4a - Jan	Ca^{2+}, $CaSO_4$, $CuCO_3$, Cu^{2+}, Mg^{2+}, $MgSO_4$, Mn^{2+}, $MnSO_4$, $PbCO_3$, Zn^{2+}, $ZnSO_4$	Cu (4.4%), Zn (0.05%)
	4a - Febr	Ca^{2+}, $CaSO_4$, $CuCO_3$, Mg^{2+}, $MgSO_4$, Mn^{2+}, Zn^{2+}, $ZnSO_4$	Cu (8.1%), Zn (0.4%), Cd (0.3%)

		Species*	
	4b - Dec	Ca^{2+}, $CaSO_4$, $CuCO_3$, Mg^{2+}, $MgSO_4$, Mn^{2+}, $MnSO_4$, $PbCO_3$, Pb^{2+}, Zn^{2+}, $ZnSO_4$	Cu (12%), Zn (0.4%), Cd (0.3%)
	4b - Jan	Ca^{2+}, $CaSO_4$, $CuCO_3$, Cu^{2+}, Mg^{2+}, $MgSO_4$, Mn^{2+}, $MnSO_4$, $PbCO_3$, Pb^{2+}, Zn^{2+}, $ZnSO_4$	Cu (5.8%), Zn (0.06%)
	4b - Febr	Ca^{2+}, $CaSO_4$, $CuCO_3$, Mg^{2+}, $MgSO_4$, Mn^{2+}, $MnSO_4$, Zn^{2+}, $ZnSO_4$	Cu (12%), Zn (0.4%), Cd (0.3%)
	4c - Dec	Ca^{2+}, $CaSO_4$, $CuCO_3$, Mg^{2+}, $MgSO_4$, Mn^{2+}, $MnSO_4$, $PbCO_3$, Pb^{2+}, Zn^{2+}, $ZnSO_4$	Cu (13%), Zn (0.6%)
	4c - Jan	Ca^{2+}, $CaSO_4$, $CuCO_3$, Mg^{2+}, $MgSO_4$, Mn^{2+}, $MnSO_4$, $PbCO_3$, Pb^{2+}, Zn^{2+}, $ZnSO_4$	Cu (2.7%), Zn (0.2%)
	4c - Febr	Ca^{2+}, $CaSO_4$, $CdCl^+$, Cd^{2+}, $CuCO_3$, Mg^{2+}, $MgSO_4$, Mn^{2+}, $MnSO_4$, $PbCO_3$, Zn^{2+}, $ZnSO_4$	Cu (9.7%), Zn (0.4%), Cd (0.2%), Pb (1.2%)
	5a+5b - Dec	Ca^{2+}, $CaSO_4$, $CuOH^+$, $CuCO_3$, Mg^{2+}, $MgSO_4$, Mn^{2+}, $MnSO_4$, $PbCO_3$, Zn^{2+}, $ZnSO_4$	Cu (66%), Zn (4%), Pb (0.05%)
	5a - Jan	Ca^{2+}, $CaSO_4$, $CuCO_3$, $CuOH^+$, Cu^{2+}, Mg^{2+}, $MgSO_4$, Mn^{2+}, $MnSO_4$, $PbCO_3$, Pb^{2+}, Zn^{2+}, $ZnSO_4$	no O.C.
	5a - Febr	Ca^{2+}, $CaSO_4$, $CdCl^+$, Cd^{2+}, $CuCO_3$, Mg^{2+}, $MgSO_4$, Mn^{2+}, $MnSO_4$, $PbCO_3$, Zn^{2+}, $ZnSO_4$	Cu (22%) Zn (1%), Cd (0.7%), Pb (2%)
	5b - Jan	Ca^{2+}, $CaSO_4$, $CuCO_3$, $CuOH^+$, Mg^{2+}, $MgSO_4$, Mn^{2+}, $MnSO_4$, $PbCO_3$, Pb^{2+}, Zn^{2+}, $ZnSO_4$	Cu (0.06%), Zn (0.3%)
P9	5b - Febr	Ca^{2+}, $CaSO_4$, $CdCl^+$, Cd^{2+}, $CuCO_3$, Mg^{2+}, $MgSO_4$, $PbCO_3$, Zn^{2+}, $ZnSO_4$	Cu (22%), Zn (1%), Cd (0.7%), Pb (2%)
	ryzhom 19 Apr	Ca^{2+}, $CaSO_4$, $CdCl^+$, Cd^{2+}, Mg^{2+}, $MgSO_4$, $PbCO_3$, $PbOH^+$, Pb^{2+}, Zn^{2+}, $ZnSO_4$	Zn (2.8%), Cd (1.3%), Pb (5.6%)
	ryzhom 22 Apr	Ca^{2+}, $CaSO_4$, $CdCl^+$, Cd^{2+}, Mg^{2+}, $MgSO_4$, Mn^{2+}, $MnSO_4$, $PbCO_3$, $PbOH^+$, Pb^{2+}, Zn^{2+}, $ZnSO_4$	Zn (2.3%), Cd (1.3%), Pb (4%)
	ryzhom 25 Apr	Ca^{2+}, $CaSO_4$, $CdCl^+$, Cd^{2+}, $CuCO_3$, Mg^{2+}, $MgSO_4$, Mn^{2+}, $MnSO_4$, $PbCO_3$, $PbOH^+$, Pb^{2+}, Zn^{2+}, $ZnSO_4$	Zn (2.3%), Cd (0.6%), Pb (37%)
	lysim 25 Apr	Ca^{2+}, $CaSO_4$, $CdCl^+$, Cd^{2+}, $CuCO_3$, Mg^{2+}, $MgSO_4$, Mn^{2+}, $MnSO_4$, Zn^{2+}, $ZnSO_4$	Cu (94%), Zn (3%), Cd (0.9%)

*listed for each element in order of relative abundance; only species present in amounts >5% are reported
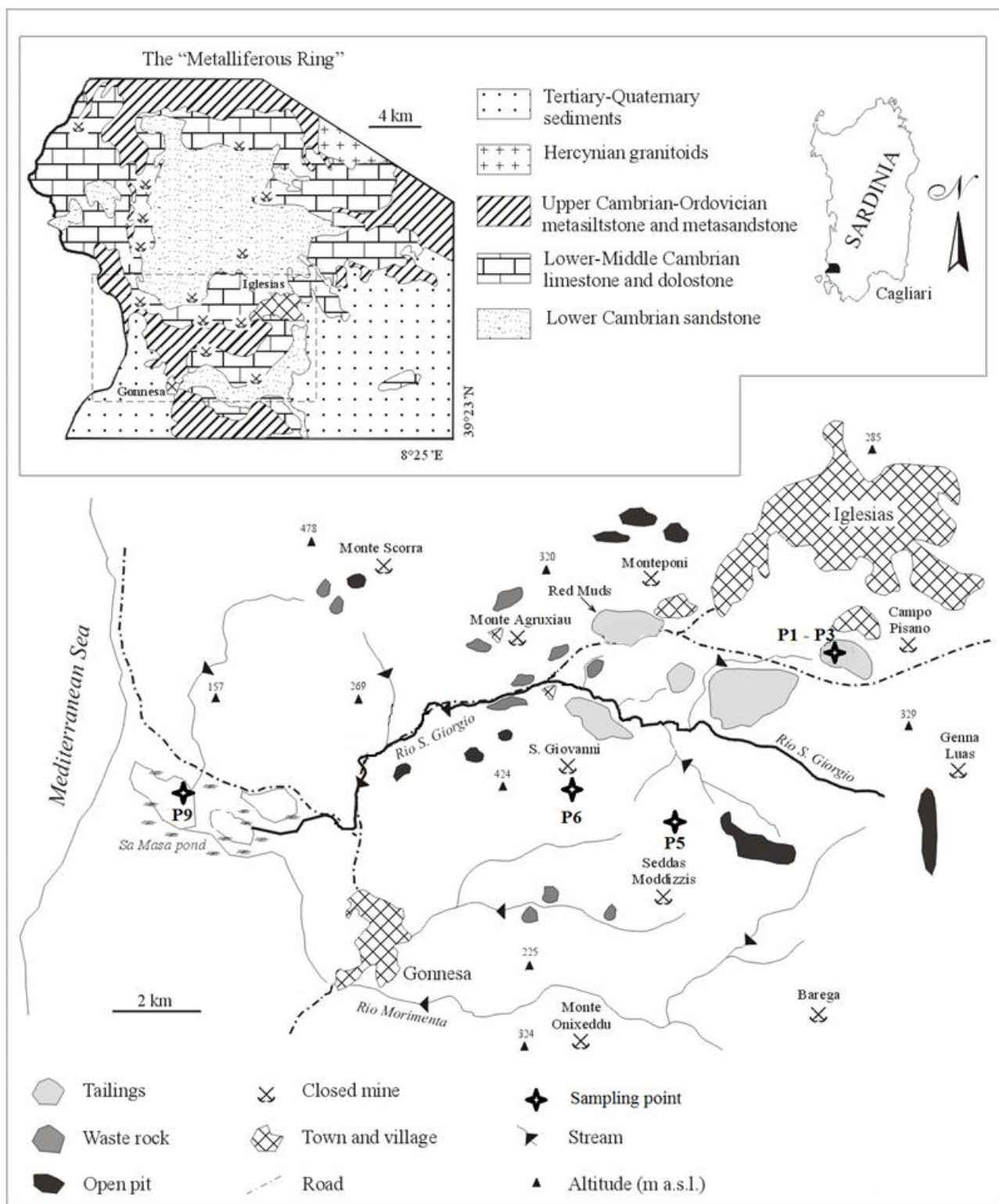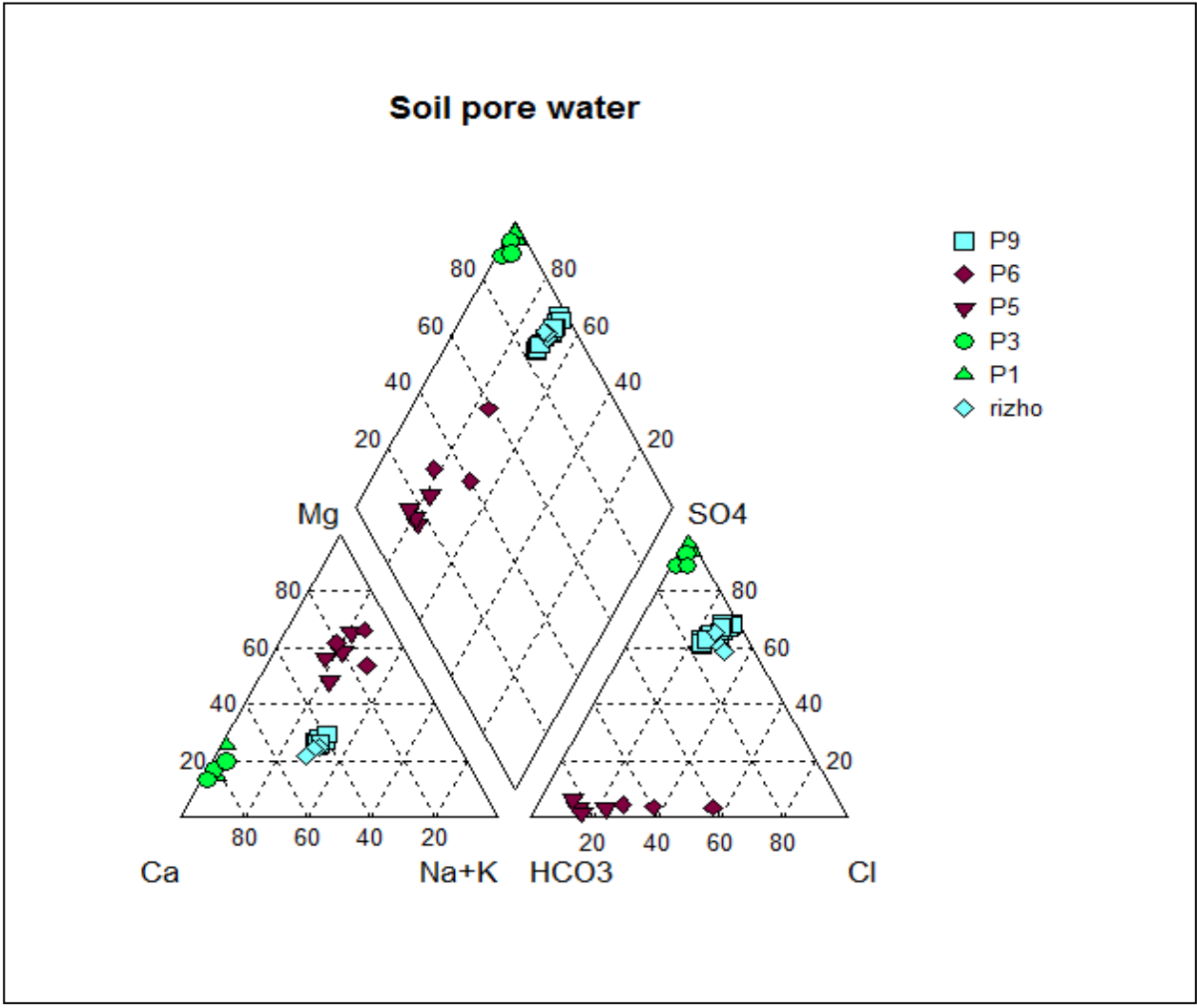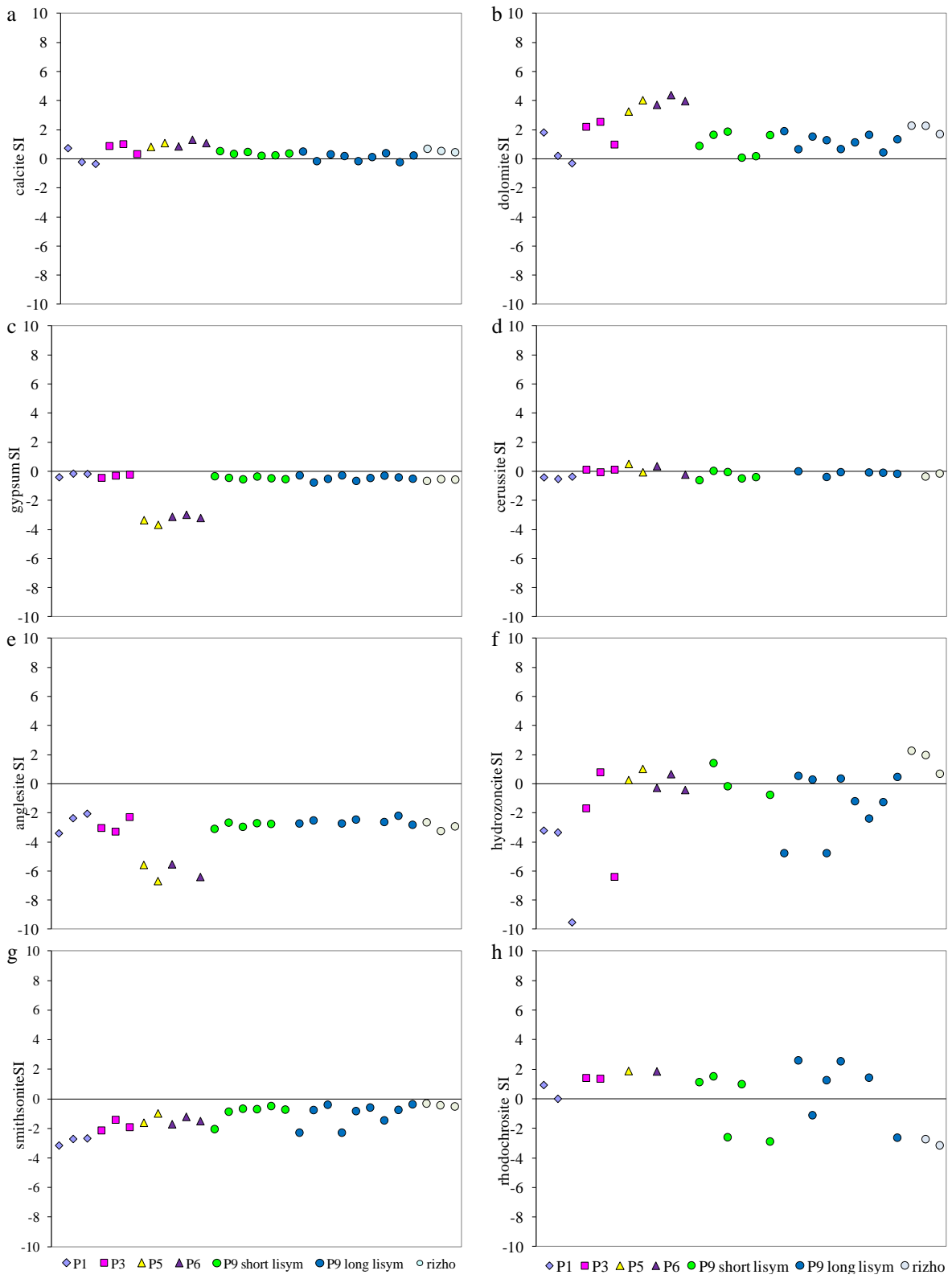
Table 5.

Figure

Fig. 1

Fig 2

Figure

Fig. 3

Figure

Fig. 4

Figure

Fig. 5